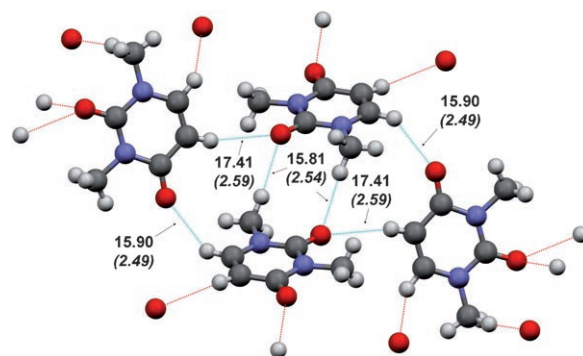


# Probing Noncovalent Interactions in Biomolecular Crystals with Terahertz Spectroscopy

Thomas Kleine-Ostmann,<sup>[b, d]</sup> Rafal Wilk,<sup>[b]</sup> Frank Rutz,<sup>[b, e]</sup> Martin Koch,<sup>[b]</sup> Henning Niemann,<sup>[c]</sup> Bernd Güttler,<sup>[c]</sup> Kai Brandhorst,<sup>[a]</sup> and Jörg Grunenberg<sup>\*[a]</sup>

The far-infrared vibrational spectra of molecular crystals are dominated by intramolecular (internal) modes, which are also present in the isolated molecule, and noncovalent intermolecular modes, which arise from the interaction of the nearest neighbours (external modes). Conceptually this has long been understood and early experiments<sup>[1]</sup> using Fourier transform infrared (FTIR) spectroscopy confirmed the existence of a rich vibrational spectrum in polypeptides in the low-energy region. Yet, the assignment of the experimentally observed peaks in the low-energy region is often unsatisfying. Recently, the advent of terahertz time-domain spectroscopy (THz TDS) has revitalized the field. Using this convenient room-temperature technique, noncovalent interactions between several small- and medium-sized molecules have been investigated, including nucleobases and nucleosides,<sup>[2–4]</sup> short-chain polypeptides,<sup>[5]</sup> cystine and glutathione,<sup>[6]</sup> retinal,<sup>[7]</sup> and saccharides.<sup>[8]</sup> Chen et al.<sup>[9]</sup> and Nagai et al.<sup>[10]</sup> could clearly distinguish between intramolecular and intermolecular modes by comparing crystalline structures and solvated molecules. Furthermore, it was shown that different isomers<sup>[7]</sup> as well as diverse crystalline forms<sup>[11]</sup> show distinctively different terahertz spectra. Most of these experiments have benefited from a comparison with quantum-mechanical calculations of the normal modes, which are nowadays feasible due to advances both in computer technology and software development.

Herein, we study two types of molecular crystals—one with weak [dimethyluracil (DMU), see Figure 1] and one with strong hydrogen bonds [thymine (THY), see Figure 2]. In order to gain insight into the chemical nature of the THz signals by assigning individual low-frequency modes, we compare our data to a



**Figure 1.** Arrangement of 1,3-dimethyluracil (DMU) in the unit cell. Hydrogen bonds are indicated as dashed lines. Theoretical compliance constants and the corresponding interatomic distance (in brackets) are given in units of Åmdyne<sup>−1</sup> and Å, respectively.

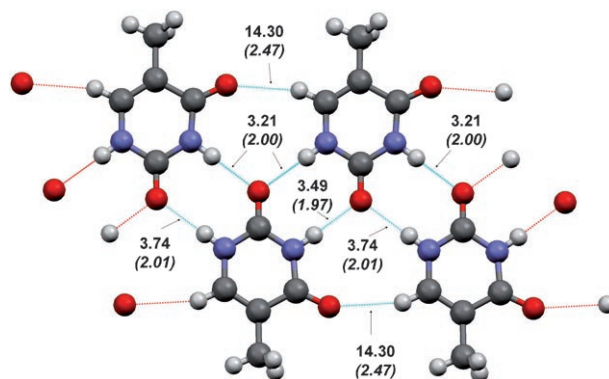


**Figure 2.** Arrangement of thymine (THY) molecules in a unit cell. Hydrogen bonds are indicated as dashed lines. Theoretical compliance constants and the corresponding interatomic distance (in brackets) are given in units of Åmdyne<sup>−1</sup> and Å, respectively.

systematic set of DFT calculations performed for molecular clusters of different sizes.

In principle, there are two possible ways to model the effect of crystal packing in theoretical vibrational studies. On the one hand, if the interactions in the system are uniform and long-range, one has to calculate an infinite three-dimensional crystal using periodic boundary conditions (PBC).<sup>[12]</sup> Metals and systems with relatively small band gaps such as conjugated polymers are typical examples where this type of calculation is inevitable. Nevertheless, most calculations using periodic boundary conditions are hampered by the fact that—due to time demands—dipole moment derivatives are determined at lower levels of theory.<sup>[13–15]</sup> On the other hand, cluster calculations

- [a] K. Brandhorst, Dr. J. Grunenberg  
Institut für Organische Chemie, Technische Universität Braunschweig  
Hagenring 30, 38106 Braunschweig (Germany)  
Fax: (+49)-531-391-5388  
E-mail: Joerg.Grunenberg@tu-bs.de
- [b] Dr. T. Kleine-Ostmann, Dr. R. Wilk, Dr. F. Rutz, Prof. Dr. M. Koch  
Institut für Hochfrequenztechnik, Technische Universität Braunschweig,  
Schleinitzstraße 22  
38106 Braunschweig (Germany)  
Fax: (+49)-531-391-2045
- [c] H. Niemann, Prof. Dr. B. Güttler  
Physikalisch-Technische Bundesanstalt, Bundesallee 100, 38116 Braunschweig (Germany)
- [d] Dr. T. Kleine-Ostmann  
Physikalisch-Technische Bundesanstalt, Working Group Electromagnetic Fields  
Bundesallee 100, 38116 Braunschweig (Germany)
- [e] Dr. F. Rutz  
Fraunhofer Institut für Angewandte Festkörperphysik  
Tullastr. 72, 79108 Freiburg (Germany)

beginning with an isolated monomer and adding successively more moieties allow for 1) straightforward discrimination between intra- and intermolecular (phonon) vibrations and 2) the accurate calculation of dipole moment derivatives, that means infrared intensities. Such a cluster approach should be successful in cases where chemical bonds are well localized. It is actually inevitable if the long-range order of the crystal is destroyed. Herein we follow the cluster approach as we are interested in the individual interactions of the molecular moieties with its nearest neighbours on an atomic scale.

Generally, the noncovalent interactions between the moieties that hold a molecular crystal together can be numerous or less numerous on one hand, and weak and strong on the other hand. While, for example, conventional hydrogen bonds ( $\text{O}\cdots\text{H}\cdots\text{O}$ ,  $\text{N}\cdots\text{H}\cdots\text{O}$ ,  $\text{N}\cdots\text{H}\cdots\text{N}$  and  $\text{O}\cdots\text{H}\cdots\text{N}$ ) have a binding strength of  $\sim 4\text{--}6\text{ kcal mol}^{-1}$  [16,17] and a mechanical strength measured by a compliance constant of  $\sim 3\text{--}7\text{ Åmdyne}^{-1}$  [18] most  $\text{C}\cdots\text{H}\cdots\text{O}$  interactions are much weaker with a binding strength of  $\sim 1\text{--}2\text{ kcal mol}^{-1}$  [19] and a compliance constant higher than  $15\text{ Åmdyne}^{-1}$  [18]. The relative weakness of hydrogen bonds in comparison with a typical covalent bond (e.g. a  $\text{C}\cdots\text{C}$  single bond with  $0.2\text{ Åmdyne}^{-1}$  [20]) should make a decomposition of the vibrational spectrum into internal and external (lattice) modes a justifiable approximation.

Experimental room temperature THz spectra for thymine are available in the literature. [2,21] They have been obtained with THz time-domain [2] and FTIR spectroscopy. [21] To obtain experimental THz spectra for dimethyluracil we use the same experimental techniques. We use a standard time-domain THz spectrometer with photoconductive dipole antennas to cover the frequency range between 100 GHz to 2 THz. For higher frequencies we use a standard FTIR spectrometer (Bio-Rad FTS 40 V) in conjunction with a helium cooled bolometer as detector element. Dimethyluracil came in powder form. Following the standard procedure the powder was mixed with polyethylene (Merck Uvasol) and pressed into a thin pellet. Our cluster calculations are based on a density functional theory (DFT) using the B3LYP hybrid density functional [22] and a standard double-zeta basis set augmented with one set of polarization functions [6-31G(d)]. This combination produces reliable force fields not only for covalent bonds but also for weaker interactions like hydrogen bonds. All starting cluster geometries were taken from solid-state X-ray measurements and were subject to structural optimizations. After the RMS gradient reached  $1\times 10^{-4}\text{ au}$ , all energy minimizations were stopped. The calculations of vibrational frequencies were done using analytical energy second derivatives while intensities were computed using the dipole moment derivatives. No scaling of the obtained results was done.

For each substance we systematically model the isolated molecular moieties, followed by the dimer, trimer and higher clusters. All computations were done using the Gaussian03 program set. [23] The experimental data are shown in Figures 3 and 4. The upper two plots (a+b) show the experimental data. On the left we plot the lower THz TDS data with frequencies up to 1.5 THz and 3.5 THz, respectively. The upper THz data for frequencies between 1.5 THz and 15 THz are shown

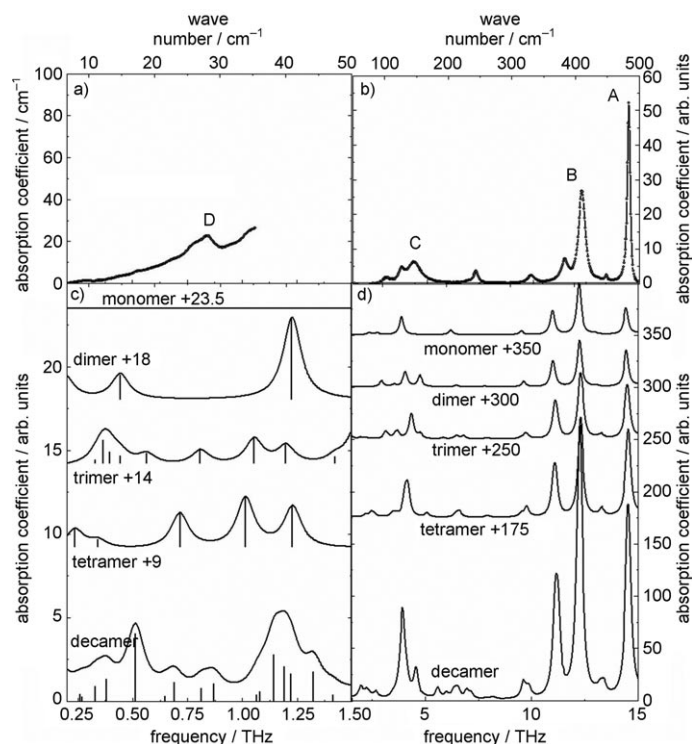


**Figure 3.** Measured absorption coefficient of dimethyluracil (DMU) in the frequency range of a) 200 GHz to 1.5 THz and b) 1.5 THz to 15 THz in comparison to the calculated absorption coefficient in the frequency range of c) 200 GHz to 1.5 THz and d) 1.5 THz to 15 THz. The calculated absorption coefficients are offset for clarity.

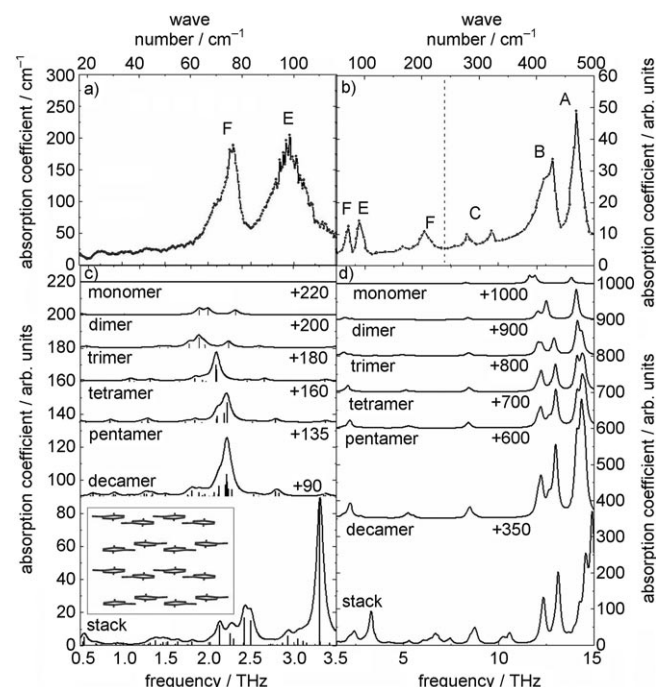


**Figure 4.** Measured absorption coefficient of thymine (THY) in the frequency range of a) 500 GHz to 3.5 THz (from [2]) and b) 1.5 THz to 15 THz [21] in comparison to the calculated absorption coefficient in the frequency range of c) 500 GHz to 3.5 THz and d) 1.5 THz to 15 THz. The calculated absorption coefficients are offset for clarity.

on the right side. The corresponding theoretical curves are displayed in the lower part of the figures (c + d). In order to make the theoretical line spectra comparable to the experiment, the calculated line peaks are broadened by Lorentzian lines with a full-width at half maximum of 100 GHz and 250 GHz for the lower and higher frequency window, respectively. These values correspond to those observed experimentally. The experimentally observed linewidths are not limited by the resolution of the spectrometers. The observation of somewhat broader linewidths in the higher frequency window may arise from the fact that the vibrational energy in these resonances can relax via anharmonic coupling into vibrations at lower frequencies whereas less relaxation channels exist for the vibrations in the lower frequency window. A detailed study of this effect is, however, not within the scope of this paper.

As a prototype for a molecular crystal which contains exclusively weak C—H...O hydrogen bonds (four per moiety) between nearest neighbors, we choose 1,3-dimethyluracil (see Figure 1 for a three-dimensional representation). Preliminary compliance constants calculations for the intermolecular C—H...O hydrogen bridges for the DMU oligomers indeed point to a very shallow curvature for the intermolecular potential. For example the DMU decamer calculations reveal C—H...O compliance constants between  $15.8 \text{ Å mdyne}^{-1}$  and  $17.4 \text{ Å mdyne}^{-1}$  (B3LYP/dz level of theory) for the central DMU dimeric unit (see Figure 1). Note, that a higher compliance constant corresponds to a weaker interaction. This type of weak intermolecular hydrogen bonds should in principle give rise to signals, particularly in the lower THz region, provided that the transition dipole moment for those normal modes is large enough. From Figure 3, which shows a comparison between theory and experiment for DMU, we draw the following conclusions:

- 1) In the upper THz region, the theoretical spectrum calculated for the monomer is already very similar to the experimental curve. The agreement converges quickly if more neighbours are considered.
- 2) The strong peaks in the upper THz region between 12.5 THz and 15 THz (A and B) originate from intramolecular vibrations, since the spectral positions of the peaks do not shift noticeably going from the mono- to the decamer. A normal mode analysis of our DMU decamer cluster indeed reveals that these signals are due to localized C=O in-plane bending and internal ring breathing, respectively, which are only weakly influenced by intermolecular forces.
- 3) Turning to the lower THz region, the calculation of the isolated monomer does not predict any peaks below 1.5 THz. The only feasible intramolecular mode for DMU in this energy region, the methyl rotation, is hindered due to weak intramolecular  $C_{\text{Meth}}\text{H}\cdots\text{O}=\text{C}$  hydrogen contacts. This resonance is therefore shifted into the upper THz region (C), suggesting that the experimentally observed peak around 0.8 THz (D) results exclusively from long-range intermolecular vibrations. Yet, an assignment of this peak is hardly possible because—in contrast to the upper THz region—the pattern resulting from our simulation of the

lower THz spectrum is still not converged using ten individual DMU moieties. Nevertheless, based on a normal mode analysis of our DMU decamer cluster, all theoretical peaks below 1.5 THz can be described as translational and librational motions of rigid DMU moieties. Hence, they are strictly external by nature.

In contrast to DMU, thymine, one of the nucleobases in DNA, is able to build strong N—H...O hydrogen bonds to its next neighbors. Due to our compliance constants calculation the mechanical strength of the N—H...O hydrogen bonds in thymine is between  $3.2 \text{ Å mdyne}^{-1}$  and  $3.7 \text{ Å mdyne}^{-1}$ , depending on the position of the hydrogen bond (see Figure 2). Assisted by weaker C—H...O hydrogen bonds, which are again in the range between  $14 \text{ Å mdyne}^{-1}$  and  $17 \text{ Å mdyne}^{-1}$ , thymine forms a layer structure of planar poly-thymine sheets. From the comparison of the experimental THz spectrum with the simulated spectra for the mono- up to the 16 mer (Figure 4), we conclude the following:

- 1) For both energy ranges, the upper and the lower THz region, the agreement considerably improves and converges quickly as more and more nearest neighbours are considered.
- 2) Due to our normal mode analysis of the cluster simulation, the strong peaks in the upper THz region (A and B) above 12 THz (C=O in-plane bending and ring breathing) are, as in the case of DMU, dominated by intramolecular interactions. In contrast to DMU the perturbation due to the next neighbours mediated by strong N—H...O hydrogen bonds is pronounced. When going from the mono- to the 16 mer these peaks blueshift up to  $\sim 40 \text{ cm}^{-1}$ .
- 3) The weak resonance around 10 THz (C) is caused by an intramolecular (in-plane) bending of the methyl groups, while the peak at 6 THz (D) is already dominated by an intermolecular motion, namely the rigid body in-plane librational modes of individual thymine molecules. The energy of this mode is determined by the relatively strong N—H...O hydrogen bonds, which have to be broken partially during this libration.
- 4) For thymine, our cluster calculation seems to have converged at the decamer cluster, also for the lower THz region, even if some of the weaker signals in the experimental spectrum, especially the peak at 3.0 THz (E) is missing.
- 5) Yet, when switching on the stacking interactions in our simulation by arranging individual sheets in a pile (inset in Figure 4), a unique assignment for both the upper and lower THz region is possible. Both experimental peaks in the lower THz region namely at  $\sim 2.25 \text{ THz}$  (F) and notable the one at 3.0 THz (E) can now be assigned to a rigid body rotational libration of entire thymine moieties. While the signal (F) is caused by weak intermolecular C—H...O hydrogen bonds *within* the thymine sheets, the libration at (E) is predominantly determined by the weak intermolecular C—H...O contacts *between* individual sheets and can there-

fore be used as an approximate measure of the  $\pi$ -stacking interaction at work in thymine.

Using the presented combination of experimental THz spectra and theoretical calculations using molecular clusters of different size it is possible to uniquely discriminate between intra- and intermolecular (phonon) vibrations in biomolecular crystals. The distinction is particularly possible in the range between 3 THz and 10 THz, where both, weak intramolecular (DMU) and strong intermolecular interactions (THY) can overlap. This sort of combined study may help to implement THz spectroscopy as a unique tool for the measurement of non-covalent interactions.

**Keywords:** computational chemistry • molecular crystals • noncovalent interactions • terahertz spectroscopy • vibrational spectroscopy

- [1] S.-C. Shen, L. Santo, L. Genzel, *Can. J. Spectrosc.* **1981**, 26, 123.
- [2] B. M. Fischer, M. Walther, P. Uhd Jepsen, *Phys. Med. Biol.* **2002**, 47, 3807.
- [3] Y. C. Shen, P. C. Upadhyaya, E. H. Linfield, A. G. Davies, *Appl. Phys. Lett.* **2003**, 82, 2350.
- [4] Y. C. Shen, P. C. Upadhyaya, E. H. Linfield, A. G. Davies, *Appl. Phys. Lett.* **2005**, 87, 011105.
- [5] M. R. Kutteruf, C. M. Brown, L. K. Iwaki, M. B. Campbell, T. M. Korter, E. J. Heilweil, *Chem. Phys. Lett.* **2003**, 375, 337.
- [6] K. Yamamoto, M. H. Kabir, K. Tominaga, *J. Opt. Soc. Am. B* **2005**, 22, 2417.
- [7] M. Walther, B. Fischer, M. Schall, H. Helm, P. U. Jepsen, *Chem. Phys. Lett.* **2000**, 332, 389.
- [8] M. Walther, B. M. Fischer, P. U. Jepsen, *Chem. Phys.* **2003**, 288, 261.
- [9] Y. Chen, H. Liu, Y. Deng, D. Schauki, M. J. Fitch, R. Osiander, C. Dodson, J. B. Spicer, M. Shur, X.-C. Zhang, *Chem. Phys. Lett.* **2004**, 400, 357.
- [10] N. Nagai, R. Kumazawa, R. Fukasawa, *Chem. Phys. Lett.* **2005**, 413, 495.
- [11] C. J. Strachan, P. F. Taday, D. A. Newnham, K. C. Gordon, J. A. Zeitler, M. Pepper, T. Rades, *J. Pharm. Sci.* **2005**, 94, 837.
- [12] For a recent example of a PBC study see: D. G. Allis, D. A. Prokhorova, T. M. Korter, *J. Phys. Chem. A* **2006**, 110, 1951.
- [13] D. G. Allis, T. M. Korter, *ChemPhysChem* **2006**, 7, 2398.
- [14] T. M. Korter, R. Balu, M. B. Campbell, M. C. Beard, S. K. Gregurick, E. J. Heilweil, *Chem. Phys. Lett.* **2006**, 418, 65.
- [15] P. Uhd Jepsen, S. J. Clark, *Chem. Phys. Lett.* **2007**, 442, 275.
- [16] G. A. Jeffrey, *An Introduction to Hydrogen Bonding*, Oxford Univ. Press, Oxford, **1997**.
- [17] A. Asensio, N. Kobko, J. J. Dannenberg, *J. Phys. Chem. A* **2003**, 107, 6441.
- [18] a) J. Grunenberg, *J. Am. Chem. Soc.* **2004**, 126, 16310; b) S. S. Zhu, H. K. Brandhorst, J. Grunenberg, F. Gruppi, E. Dalcanele, A. Lützen, K. Rissanen, C. A. Schalley, *Angew. Chem.* **2008**, *Angew. Chem. Int. Ed.* **2008**, 47, 788. For a general review on compliance constants see K. Brandhorst, J. Grunenberg, *ChemPhysChem* **2007**, 8, 1151.
- [19] E. Arbely, I. T. Arkin, *J. Am. Chem. Soc.* **2004**, 126, 5362.
- [20] J. Grunenberg, *Angew. Chem.* **2001**, 113, 4150; *Angew. Chem. Int. Ed.* **2001**, 21, 4027.
- [21] S. L. Zhang, K. H. Michaelian, G. R. Loppnow, *J. Phys. Chem. A* **1998**, 102, 461.
- [22] A. D. Becke, *J. Chem. Phys.* **1992**, 97, 9173.
- [23] GAUSSIAN 03 (Revision B.02) M. J. Frisch, G. W. Trucks, H. B. Schlegel, G. E. Scuseria, M. A. Robb, J. R. Cheeseman, J. A. Montgomery, Jr., T. Vreven, K. N. Kudin, J. C. Burant, J. M. Millam, S. S. Iyengar, J. Tomasi, V. Barone, B. Mennucci, M. Cossi, G. Scalmani, N. Rega, G. A. Petersson, H. Nakatsuji, M. Hada, M. Ehara, K. Toyota, R. Fukuda, J. Hasegawa, M. Ishida, T. Nakajima, Y. Honda, O. Kitao, H. Nakai, M. Klene, X. Li, J. E. Knox, H. P. Hratchian, J. B. Cross, C. Adamo, J. Jaramillo, R. Gomperts, R. E. Stratmann, O. Yazyev, A. J. Austin, R. Cammi, C. Pomelli, J. W. Ochterski, P. Y. Ayala, K. Morokuma, G. A. Voth, P. Salvador, J. J. Dannenberg, V. G. Zakrzewski, S. Dapprich, A. D. Daniels, M. C. Strain, O. Farkas, D. K. Malick, A. D. Rabuck, K. Raghavachari, J. B. Foresman, J. V. Ortiz, Q. Cui, A. G. Baboul, S. Clifford, J. Cioslowski, B. B. Stefanov, G. Liu, A. Liashenko, P. Piskorz, I. Komaromi, R. L. Martin, D. J. Fox, T. Keith, M. A. Al-Laham, C. Y. Peng, A. Nanayakkara, M. Challacombe, P. M. W. Gill, B. Johnson, W. Chen, M. W. Wong, C. Gonzalez, J. A. Pople, Gaussian, Inc., Pittsburgh PA, **2003**.

Received: October 31, 2007

Published online on February 13, 2008